The importance of surface chemistry in mesoporous materials: lessons from porous silicon biosensors

Kristopher A. Kilian, Till Böcking and J. Justin Gooding*

Received (in Cambridge, UK) 4th September 2008, Accepted 25th September 2008
First published as an Advance Article on the web 30th October 2008
DOI: 10.1039/b815449j

The ease of fabricating high quality photonic crystals from porous silicon and its biocompatibility have inspired the conception of various biosensing schemes using this material. However, the instability of porous silicon has significantly slowed progress in this area. Here we discuss the potential of different porous silicon photonic crystals for biosensing in the context of its surface chemistry and nanostructure, both of which need to be optimized to obtain sensitive and stable devices. Of particular promise are recent approaches that use porous silicon as sensors for enzymatic activity, for cell capture and concentration devices.

Introduction

Porous silicon (PSi) was discovered by Uhlir and others at Bell labs in the 1950s when a reddish-brown colour appeared on silicon during attempts at electropolishing.[1] Initially attributed to a suboxide species, PSi attracted very little scientific attention until two key discoveries by Canham and co-workers. The first in 1990 was the prediction and then demonstration of room temperature photoluminescence from the material that was easily tunable making PSi a promising material for optoelectronics.[2] The second was a 1995 report that PSi has potential as a tunable biomaterial, which facilitates hydroxyapatite growth and/or degrades to benign products (silylic acid) after exposure to physiological fluids.[3] Equally seminal for the field was the demonstration by Vincent in 1994 that the refractive index of PSi could readily be tuned during fabrication to produce one-dimensional photonic crystals.[4] As a consequence, research into the properties of PSi gained considerable momentum as an attractive candidate material for optoelectronics, photonics and biological applications.

With the ability of porous silicon to be both a photonic device and a biocompatible material, application in biosensing was almost inevitable. Sailor, Ghadiri and colleagues first reported the use of mesoporous PSi thin films for interferometric detection of biological recognition.[5] Since this report, many groups have employed a wide array of different optical structures formed with PSi to select and detect a variety of biological molecules (see for example refs. 6–11).

It is clear from the majority of research that a key challenge to effectively use PSi in biosensing is the stabilization of the structure *via* appropriate surface chemistry. This is a challenge that has recently become the focus of much attention with strategies being developed that allow unprecedented stability of the material during experiments in biological solutions.[7,8,12–15]

School of Chemistry, The University of New South Wales, NSW 2052 Sydney, Australia. E-mail: Justin.gooding@unsw.edu.au; Fax: 61 2 9385 6141; Tel: +61 2 9385 5384

Kristopher A. Kilian

Kristopher Kilian received Bachelor and Masters degrees in chemistry from the University of Washington. He did his PhD work with Justin Gooding at the University of New South where he investigated chemical modification of nanostructured silicon optical materials for biomedical applications. Kris's research interests include surface chemistry, nano- and micro-engineering and interfacing synthetic materials with live biological systems. He is currently a Howard Hughes Medical Institute post-doctoral associate in the laboratory of Milan Mrksich at the University of Chicago where he investigates model surfaces for studying cells and tissue.

Till Böcking

Till Böcking completed his undergraduate degree in biology at the University of Bonn followed by a PhD in biophysics under the guidance of Hans Coster and Kevin Barrow at the University of New South Wales. Afterwards he was recruited to the groups of Justin Gooding and Michael Gal to apply his expertise in silicon surface chemistry to the porous silicon biosensor project. He is currently a post-doctoral researcher at Harvard Medical School with a Cross-disciplinary fellowship of the Human Frontier Science Program where he is interested in using modified surfaces and materials to study biological processes at the single molecule level.

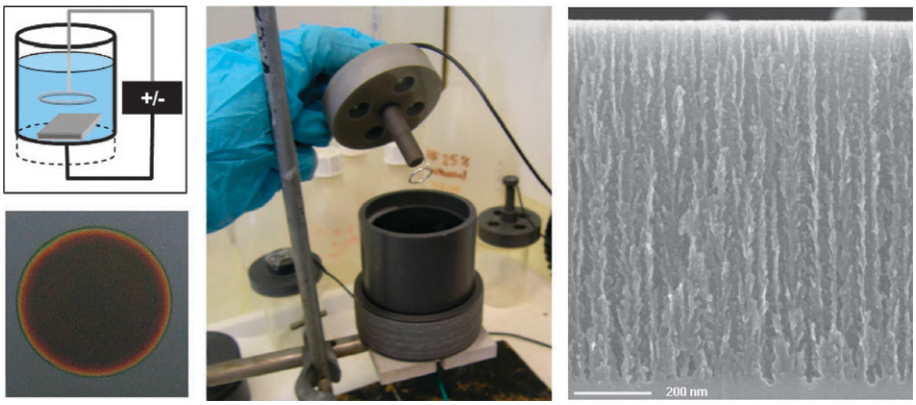

Fig. 1 Upper left/middle: Schematic and photograph of the electrochemical etching cell used for anodization of silicon. Lower left: Photograph of a Bragg mirror photonic crystal etched in this apparatus. Right: Cross-sectional view scanning electron micrograph (SEM) of a thin layer of PSi etched under conditions to yield a branched, columnar pore morphology running perpendicular to the surface.

This article reviews the past and present of using this material for biosensing and how advances in surface chemistry are opening up many new and exciting possibilities for using PSi for diagnostic devices. The first three sections review PSi formation, surface chemistry and biosensing respectively with a focus on the importance of surface chemistry and tuning pore morphology. In the last section we highlight lessons learned from our work and the importance of understanding the surface chemistry with respect to the internal geometry to effectively implement PSi in biosensing applications.

1. Porous silicon formation

There are numerous methods and mechanisms for PSi formation, the bulk of which can be classified as electrochemical, photoelectrochemical and 'stain etching' methods that do not require light or electrical bias.[16] Anodisation under galvanostatic conditions is by far the most commonly used method (Fig. 1). Both phosphorous (n-type) and boron (p-type) doped silicon can be electrochemically etched in aqueous and/or organic electrolyte solutions containing HF to yield a range of nano- to micro-scale structures by simply selecting the appropriate dopant concentration of the Si substrate and/or adjusting the anodisation conditions.[17] Thus, extensive research has gone into establishing conditions to fabricate PSi materials with a range of pore morphologies and pore sizes. PSi can be classified according to its pore sizes as macroporous (pore diameter $d > 50$ nm), mesoporous (2 nm $< d <$ 50 nm) and microporous ($d < 2$ nm).[18] For PSi to be amenable to optical biosensing, the size of the pores must allow infiltration of biomolecules. Therefore, biosensing efforts have focused primarily on mesoporous silicon to accommodate biological species.[15] Transduction of the biorecognition event is generally based on changes in the optical thickness caused by the adsorption or desorption of biological molecules from the surface of the pores of the PSi optical sensor. These changes in average refractive index are detected by changes in the optical signature of the PSi photonic crystal as discussed in section 3. For detailed reviews of PSi formation, characterisation and properties, the reader is referred to refs. 16, 18 and 19.

J. Justin Gooding

J. Justin Gooding is the leader of the Biosensor and Biodevices Research Group at The University of New South Wales. He obtained a DPhil from Oxford University under the guidance of Prof Richard Compton before becoming a post-doctoral research associate at the Institute of Biotechnology at Cambridge University. In 1997 he returned to his native Australia as a Vice-Chancellor Post-Doctoral Research Fellow at the University of New South Wales before taking up an academic position in 1998. He was promoted to full Professor in 2005. His research interests lie in biosensors, biointerfaces and surface chemistry.

2. Building a biorecognition interface in nanostructured silicon

An exceedingly important aspect of a biosensor's design is the biorecognition interface. The essential feature of such an interface is its ability to selectively recognise and bind the species of interest whilst preventing reactions with interfering molecules. These interfering species can either bind non-specifically and result in a false positive signal or degrade the performance of the sensor by reacting with the sensor material and changing its chemical composition. The latter aspect is a particular challenge for PSi photonic crystal based biosensors. The silicon hydride (Si–H_x, $x = 1$, 2 and 3) terminated pore walls of freshly prepared PSi are prone to oxidation under ambient conditions (atmospheric oxygen and water) and when exposed to aqueous solutions ultimately leading to dissolution of the PSi matrix (Fig. 2(i)). Oxidation of silicon causes a large change in the refractive index of the material ($n = 3.5$ for silicon, $n = 1.4$ for silicon dioxide) and thus interferes with signal transduction in PSi optical biosensors. Dissolution in

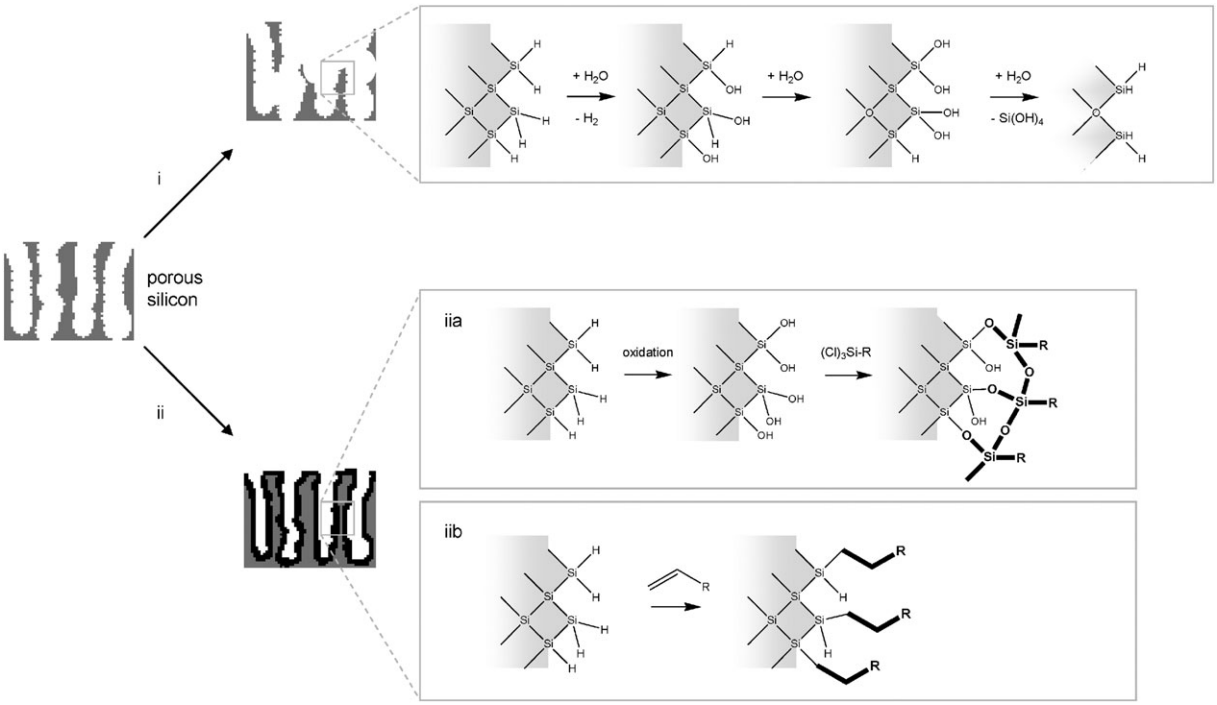

Fig. 2 (i) Depiction of porous silicon oxidation and corrosion in alkaline solutions.[22] (ii) Modification of PSi with organic monolayer *via* (iia) deliberate oxidation followed by silanization or (iib) hydrosilylation of alkenes with hydride-terminated PSi to render the surface inert.

aqueous buffers leads to an even greater change in refractive index (n = 3.5 for silicon, n = 1.33 for water) and ultimately to loss of signal due to structural collapse of the PSi thin film.[20–22] Consequently, the surface of PSi must be stabilised for applications in biological media.

A common method to stabilise porous silicon from degradation is to intentionally grow an oxide layer on the surface to slow further oxidation and avoid rapid changes in the refractive index during sensing.[23] To provide greater stability and protection against dissolution, the oxidised surface is chemically modified with alkyl silanes to form a dense monolayer that limits the access of water to the underlying surface (Fig. 2(iia)). As with other monolayer chemistries, reactive groups at the distal end of the silanes provide attachment points for biorecognition molecules. Silanization of oxidised porous silicon has been used to create biorecognition interfaces composed of DNA,[5,24–26] antibodies,[27–29] enzymes[30–33] and small molecules.[6,10] Silane chemistry is however not ideal. For many applications a pre-oxidation step is unfavourable and can negatively impact the structural and optical characteristics of the material. Furthermore, silanes tend to form multilayers if careful attention is not paid to reaction conditions. Finally due to the polarity of the Si–O–Si bond it is prone to hydrolysis under aqueous conditions such that the surface is not effectively passivated from water attacking the underlying structure and changing the optical properties of the material.[26,34]

An alternative surface chemistry is hydrosilylation of alkenes and alkynes at the hydride-terminated PSi surface resulting in the formation of a monolayer of alkyl chains linked to the surface by a very stable Si–C bond (Fig. 2(iib)). Monolayers grafted in this way are not subject to multilayer formation or hydrolysis at the base.[35] Hydrosilylation of alkenes on crystalline silicon was first reported by Linford *et al.*[36,37] and has been the subject of intense interest over the past decade.[38] Hydrosilylation of alkenes on porous silicon has been reported using thermal methods,[7,8,12–15,36,39–45] alkyl peroxides,[36] carbenium cations,[46] UV irradiation,[47] visible light,[48] microwave radiation,[49] Lewis acid catalysis,[50–52] heavy metal catalysis[53] and electron beam lithography.[54] Other schemes for Si–C bond formation include aryl lithium reagents,[55] Grignard reagents[56] and anodic and cathodic electrografting.[57,58] Surprisingly, despite the advantages of Si–C linked monolayers, and the fact that the as prepared PSi already possesses the requisite Si–H_x surface, there are only a few reports related to using this chemistry to form biorecognition interfaces on PSi compared to the more common silane chemistry. Part of the reason for so few reports is due to the fact that great care is required to perform this surface chemistry effectively. Surface modification must be performed in an inert atmosphere with completely deoxygenated and dried reagents so as to prevent the formation of silicon oxides during the monolayer formation. Despite these challenges, examples of Si–C linked biorecognition interfaces formed by hydrosilylation include: DNA,[59] enzymes,[31,32] small molecules[60] and the authors' work with peptides,[7] hybrid lipid bilayer membranes,[8] proteins[14,15] and cells.[13]

3. Porous silicon optical biosensors

3.1 Fabry–Perot layers for interferometric sensing

The concept of interferometric biosensing takes advantage of the difference in the phase of light reflected at the top surface

and base of a thin film whereby its reflectance spectrum shows an interference pattern that depends on the optical thickness (product of the refractive index n and the film thickness d) of the PSi thin film. Binding of analytes to receptors immobilized on the pore walls results in an increase in the average refractive index of the material and hence an increase in the optical thickness. This increase in optical thickness is detected as a shift of the interference pattern towards higher wavelengths (red-shift) (Fig. 3(a)). In contrast to evanescent wave techniques, there is no reliance on the surface-analyte distance thereby yielding a technique with potentially greater sensitivity.

The concept of using thin PSi films for interferometric biosensing was introduced by Sailor and colleagues.[5] The PSi thin films were subjected to oxidising conditions, modified by silanization and DNA oligonucleotides or proteins. In this early work, binding of complementary species to the interface resulted in a blue-shift of the interference pattern. The blue-shift was due to the dissolution of the PSi which indicates the surface chemistry was not sufficiently passivating to prevent the degradation of the photonic crystals. With more passivating surface chemistry, red shifts in the optical signature of Fabry–Perot layers was shown for the detection of affinity interactions[61] and protein-protein interactions.[28] These early reports underscored the importance of providing a robust surface chemistry for passivation of the underlying substrate for unambiguous interpretation of optical shifts and to prevent drift in optical responses of the PSi based biosensors.

With suitable surface passivation, researchers have detected biomolecules by red-shifts in Fabry–Perot fringes for a range of analytes including complementary DNA,[62] proteins and small molecules.[63–65] Recently, Sailor and colleagues etched double layers into a silicon chip as a method for self-compensation to control for signal drift.[11] Novel built-in control systems like this, and advances in chemical passivation strategies, should allow for continued progress with PSi Fabry–Perot optical materials in biosensing. However, more sensitive transducers have been possible with multilayered PSi photonic structures.

3.2 Porous silicon photonic crystal biosensors

The refractive index of PSi is dependent on its porosity (volume ratio of air to silicon), which in turn is a function of the current density applied during formation. The duration of the current pulses during fabrication determine the layer thickness. Thus, by periodically altering the current density during anodisation, it becomes possible to produce one-dimensional photonic crystals with a periodically varying refractive index normal to the surface. The first PSi based photonic crystals were dielectric mirrors (so called Bragg reflectors) made of alternating layers of high and low refractive index.[4,66] Imposing a $\lambda/4$ condition on the optical-thickness of the mirror layers, where λ is the centre wavelength of the reflected light, gives a near 100% reflectance band (Bragg plateau) over a desired spectral region.

Optical resonant microcavities represent a second class of photonic crystals that were produced in PSi and these have received considerably more attention for biosensing applications than Bragg reflectors. A resonant microcavity is formed by breaking up the periodicity in the Bragg stack with a defect layer. Making the optical thickness of the defect layer an integer multiple of $\lambda/2$ gives rise to a sharp cavity resonance in the centre of the Bragg plateau, where light of that wavelength "resonates" and therefore does not reflect.[67] Using similar principles to biosensing with Fabry–Perot layers, changes in the refractive index within the defect layer of the microcavity (essentially an isolated Fabry–Perot layer) will cause shifts in the cavity resonance position and thus convey a biorecognition event. A narrow linewidth cavity resonance allows small shifts to be detected faithfully such that these structures have the potential for exquisite sensitivity. While it has been shown that microcavities in PSi can be produced with a sub-nanometer linewidth cavity resonance,[68] structures compatible with biosensing have not been produced to such high optical quality.

When employing PSi microcavities in biosensing, pore sizes need to be sufficiently large to allow diffusion of bioanalytes through the Bragg mirror into the defect layer. Especially the pore diameter and nanostructure of the low porosity layers of the Bragg mirror are often incompatible with the infiltration of

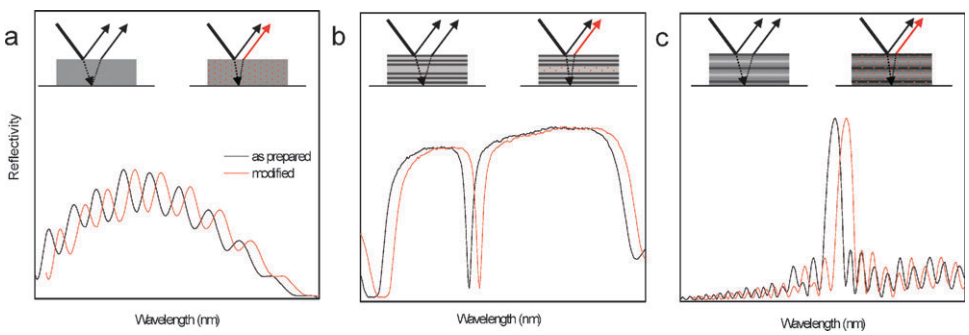

Fig. 3 (a) Schematic and spectra of a Fabry–Perot layer before (black) and after (red) modification. A change in the average refractive index of the PSi leads to a shift in the spectrum. (b) Schematic of a resonant microcavity with corresponding spectra. Each layer of alternating porosity is built with an optical thickness of $\lambda/4$ and the central defect layer with an optical thickness of $\lambda/2$, with λ being the central wavelength of the cavity resonance. (c) Schematic of a rugate filter with sinusoidal refractive index variation yielding a sharp reflectivity stop-band. The measured reflectivity of all multilayered photonic crystals arises from constructive and destructive interference from reflection at each layer (not depicted in schematic).

macromolecules. One strategy to overcome this problem is to enlarge the pores post-etch, for example by partial dissolution of the PSi in alkaline solutions.[69,70] Pore enlargement may even be necessary for biosensors for small molecules, such as glutamate, to allow introduction of the corresponding bio-recognition element, in this case glutamate binding protein, into the defect layer.[70]

While post-etch pore enlargement makes the internal pore space of the structure accessible to macromolecules, it has the disadvantage of diminishing the optical quality of the microcavity through a broadening of the cavity resonance. An alternative approach was developed by Fauchet and colleagues who conducted a systematic study to optimise anodisation parameters for the fabrication of macroporous (pore size 50–200 nm) microcavities on n-type silicon. Biosensing was demonstrated by detecting streptavidin binding to immobilised biotin ($\sim$50 pmol corresponding to 1–2% of a protein monolayer[10]). Recently, using the same n-type microcavity, Ouyang *et al.* detected $\sim$100 fmol of intimin extracellular domain binding to immobilised intimin binding domain (common recognition proteins responsible for *E. coli* pathogenicity).[71]

An important lesson arising from this work is the performance trade-offs in designing a PSi microcavity sensor. The optical quality of a microcavity can be assessed by the Q-factor, which is defined as $Q = \lambda_0/\Delta\lambda$, where λ_0 and $\Delta\lambda$ are the central wavelength and full width half maximum of the cavity resonance (or cavity line-width) respectively. To achieve high Q-value microcavities, either a high contrast between alternating layers of high and low porosity or large numbers of periods in the Bragg mirrors is required. The latter approach is less effective in porous silicon as optical scattering losses become non-negligible when large numbers of reflecting interfaces are present. However, the large jumps in porosity, and pore sizes, at the interfaces between layers of highly contrasting porosity may inhibit biomolecule diffusion. De Louise, Fauchet and colleagues attempted to alleviate this problem by making the change in porosity between layers smaller. Again, unfortunately the cost of the lower porosity difference was a significant increase in the cavity line-width which will negatively impact sensitivity of the biosensor.[10,27,71,72]

Ultimately, the type of analyte should determine the choice of micro-/nano-structural morphology when fabricating PSi photonic devices. For instance, p^+-type microcavities with a very large porosity variation between layers could be well suited for detecting small molecules (which can easily diffuse through layers) while a device for detecting macromolecules such as proteins would require a low porosity difference and relatively large pores like those observed with the n-type material.

An alternative one-dimensional photonic crystal that ameliorates some of these performance issues is the rugate filter. Rugate filters are formed by sinusoidally varying the current density during anodisation to obtain a sinusoidal refractive index profile normal to the plane of the filter (see Fig. 4). Their reflectance spectrum is characterized by a high reflectivity stop-band around a characteristic wavelength while exhibiting low reflectivity elsewhere.[73–76] Similar to resonant microcavities, changes in the optical thickness within the porous matrix upon binding of analytes cause a red-shift of the stop-band thus transducing biomolecular interactions (Fig. 3(c)).

Optimisation of the refractive index profile results in filters exhibiting a stop-band with high reflectivity and narrow line-width thus allowing sensitivity to small changes in refractive index.[73] An advantage of the rugate filter over microcavities for biosensing is the low contrast in refractive index between low and high porosity layers (1% porosity difference). Hence there is low variation in pore size which is the reason why the periodicity is not visible in the electron micrograph of a PSi rugate filter shown in Fig. 4. Because of the minor variation in pore size, biomolecular diffusion can proceed without significant changes in rate throughout the entire photonic crystal.

Sailor and co-workers have employed rugate filters with narrow linewidth stop-bands for the development of "smart dust" microparticles.[76–82] The same group used a rugate filter modified internally by electrochemical grafting of methyl groups with a thin film of protein on the surface as a device for detecting protease enzymes.[9] The authors showed that the cleavage products of the protein film gradually infiltrated into the pores of the photonic crystal, thus leading to a red-shift in the reflected light such that proteolysis could be assessed by eye from the colour change of the sensor (Fig. 5(a)). Recently, Gao and colleagues used a similar procedure with a thin layer of gelatin on a rugate filter to detect gelatinase enzymes *via* infiltration of digestion products.[83]

We have also fabricated rugate filters with narrow line-width stop-bands (full-width-half-maximum $\sim$11 nm) and high reflectivity[73] but taking a very different approach to monitoring protease activity which relied on enzymatic amplification to give a highly sensitive biosensor. Starting with our robust hydrosilylation chemistry,[84–86] to the internal surface of the rugate filters short peptides, as the biorecognition element, were covalently immobilised[7] (Fig. 5b). Digestion of the peptides immobilised on

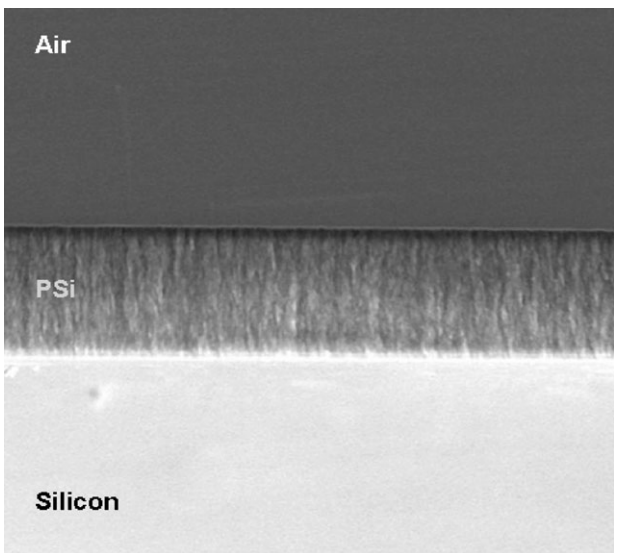

Fig. 4 Side-view scanning electron microscope image of a 40 layer rugate filter prepared on 0.07 Ω cm p^+ type Si(100) resulting in a film approximately 8.8 μm thick.

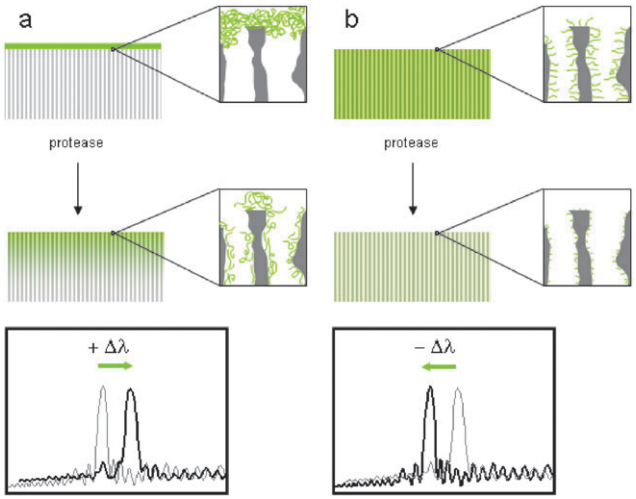

Fig. 5 Comparison of methods for protease detection using PSi rugate filters. (a) Orosco *et al.* use a thin layer of the hydrophobic protein zein on the PSi surface.[9] Exposure to protease induces cleavage and the ingress of protein fragments into the rugate filter thus causing a red-shift in the spectrum ($+\Delta\lambda$). (b) Kilian *et al.* employ covalent immobilization of peptide throughout the filter.[7] Proteolysis of the peptide at the pore walls lowers the refractive index thus resulting in a blue-shift of the reflectivity ($-\Delta\lambda$). Dimensions exaggerated for clarity.

the pore walls led to a decrease in the average refractive index and hence a blue-shift of the stop-band. As a single protease can digest many peptides inside the photonic crystal, high sensitivity was achieved with detection limits down to 7.2 pmol of enzyme. As the enzyme molecules were able to infiltrate the entire nanoporous network, the digestion of the peptide takes place uniformly throughout the photonic crystal rather than being limited to the top of the device. This "intimate mixing" of the target protease with the transducer will, in principle, allow dynamic enzyme activity assays. Importantly, using covalent immobilization of short peptides allows exquisite flexibility in choosing the substrate to suit a particular target protease enzyme. This type of sensor design is only possible, however, in the absence of signal drift and hence is only possible because of the robust surface chemical passivation strategy employed.

Throughout our work, we have found that the integrity of the surface chemistry underlying the biorecognition interface, and its relationship to the nanostructural morphology, to be critical parameters for effective use of PSi materials in biological applications. Thus we have investigated the effect of nanoarchitecture in rugate filters prepared from silicon with different doping densities on their stability and infiltration of biomolecules into these structures.[12,14,15] By optimising the structure and performance of PSi rugate filters, we have demonstrated their use as matrices for protein loading,[14] transducers of biological toxins using hybrid lipid bilayer membranes,[8] sensors for protease activity using immobilized peptides[7] and substrates for cell adhesion with the potential for detecting cellular processes.[13]

4. Tuning the biorecognition interface

4.1 Surface chemistry, stability and nanoarchitecture

In contrast to planar biosensing transducers, biorecognition in nanostructured materials is influenced by surface curvature and diffusion within nano-sized spaces. While increasing the capacity for biomolecule binding, the high surface area of nanostructured materials will also exacerbate issues of surface corrosion and false positive signals. As a consequence, having a suitable surface chemistry for protection and a detailed understanding of the PSi structure is essential.

For porous silicon devices to effectively transduce a biorecognition event the following criteria must be met: (1) the porous silicon scaffold must be protected from degradation, (2) the surface must prevent false-positives from non-specific interactions with interfering species in a complex biological sample and (3) a specific recognition moiety must be provided to bind the analyte. As discussed in section 2, hydrosilylation of ω-functionalized alkenes on PSi is a convenient route to provide a dense alkyl monolayer with very stable Si–C bonds, which fulfills the first requirement. To reduce non-specific adsorption of biomolecules, oligo(ethylene glycol) (EG) moieties can be incorporated into the monolayer by different chemical strategies.[14,86–91] To meet the third criterion, a number of different distal functionalities and corresponding coupling chemistries have been developed for covalent tethering of biorecognition molecules.

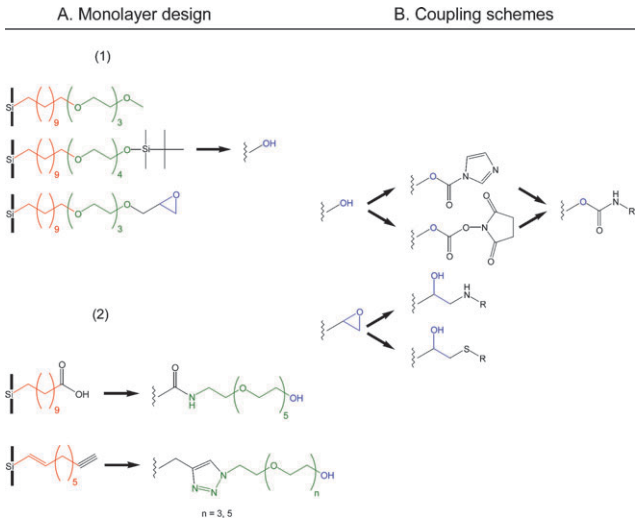

Fig. 6 A. Chemical strategies for modifying porous silicon with monolayers *via* hydrosilylation of unsaturated molecules. The aim is to stabilize the material against oxidation and corrosion with a dense alkyl layer (red), provide "anti-fouling" moieties (green) that prevent non-specific adsorption of proteins and introduce reactive groups (blue) for immobilization of receptors or enzyme substrates. (1) In the first approach the hydride-terminated PSi surface is modified in a single step with alkenes that already contain an oligo(ethylene glycol) anti-fouling moiety and reactive terminal group. (2) In the second (multi-step) strategy the PSi surface is first passivated with a short ω-functionalized alkyl monolayer, *e.g. via* hydrosilylation of an alkene (undecenoic acid) or alkyne (nonadiyne). Subsequently, an oligo(ethylene glycol) layer is linked to the alkyl layer either *via* standard coupling chemistries (activation with EDC and NHS of the terminal –COOH group) or *via* click chemistry in the case of the terminal alkyne group. B. Various coupling schemes are available to link the desired biomolecule to the reactive groups at the surface of the oligo(ethylene glycol) layer. From top to bottom: terminal hydroxide activated with either carbonyl diimidazole or disuccinimidyl carbonate. Glycidyl ether reacted directly with biological amines or thiols.

The PSi structure is prone to oxidation and collapse due to insufficient passivation[14] and physisorption of protein.[12,14,92,93] To passivate the silicon pore structure and reduce protein adsorption we explored two different strategies to covalently tether EG species to the pore walls of rugate filters. Fig. 6 shows the chemical schemes used to passivate PSi. In the first scheme (1), moieties capable of fulfilling all three criteria are built into the one alkene such that the PSi can be functionalized with the desired surface chemical properties in a single step. Using this approach, protein adsorption was reduced by 75–80% compared to a hydrophobic dodecane monolayer.[12] For creating a biorecognition interface, a series of EG molecules were synthesized that contained distal reactivity in order to covalently immobilize biological amines and thiols[84–86] (Fig. 6, coupling schemes). Unfortunately, incubation of PSi rugate filters modified with these types of monolayers in aqueous media caused a marked degradation in the modified PSi as determined by Fourier transform infrared spectroscopy (FTIR, silicon dioxide formation) and spectral reflectivity (blue-shift as a result of oxidation and structural degradation).[94] Previous studies of monolayers formed from EG functionalized alkenes on single crystal silicon(111)[86] suggested a decreased grafting density compared to unfunctionalized alkyl monolayers. It is hypothesized that this lower grafting density with EG functionalized alkenes means that the monolayer is providing an insufficient barrier to water accessing the silicon surface and hence the PSi structures degrade in aqueous media. Thus, while monolayer formation with a multifunctional species in a single step is initially attractive because its composition is well defined and not dependent on reaction yields to introduce the various functions in a stepwise manner, it does not provide the necessary passivation for mesoporous PSi biosensors.

As an alternative, a stepwise approach to fabricating the biosensing interface was employed with a base layer composed of a relatively simple alkene that would effectively passivate the PSi. First, hydrosilylation of undecenoic acid on PSi rugate filters was performed to yield monolayers with sufficiently dense alkyl chains to prevent the ingress of water to the silicon surface (Fig. 6, strategy (2)). The dense monolayer protected the PSi matrix from oxidation and structural collapse, even during subsequent chemical transformations at the monolayer surface (Fig. 7).[94,95] To add antifouling character to the interface, a 1-amino EG_6 molecule was synthesized and coupled to the NHS-ester activated surface. With this strategy protein adsorption was reduced to the same extent as observed when all components were incorporated into the one molecule as described above. Importantly, with the stepwise strategy, the surface chemistry yielded a 30-fold increase in stability when exposed to aqueous solutions.[12] Following on from the principles of this strategy, we have also investigated the Cu(I)-catalyzed alkyne-azide cycloaddition, so-called 'click' reaction, on Si(100)[96] and PSi surfaces.[97] Using a multiple-step strategy we have successfully grafted azide-terminated EG layers to dialkyne modified PSi that reduce adsorption of proteins (Fig. 6, strategy (2)). We further found that di-alkyne monolayers provide an even passivation of the silicon and provide far greater stability to aqueous media thus expanding the scope to longer exposure times in physiological environments.[98]

In addition to surface chemistry, engineering the nanoarchitecture can be used to adapt the material to suit the intended application. Our early work using p^+-type silicon (0.07 Ω cm, *medium* doped) resulted in highly branched mesopores with an average diameter of 12 nm.[14,15] As a consequence of the pore size of this material, small proteins

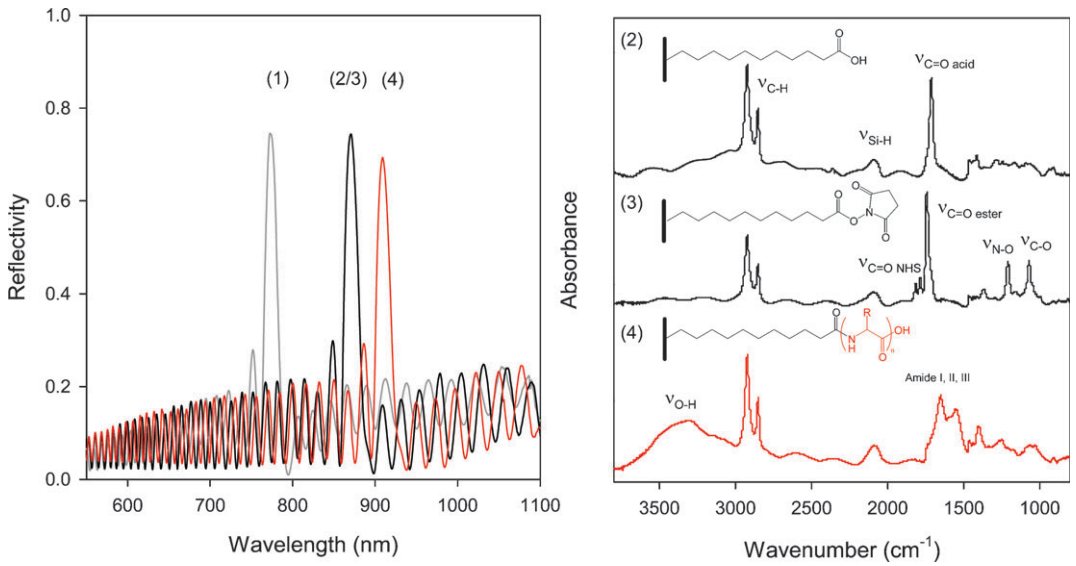

Fig. 7 Spectroscopic characterization of chemically modified rugate filters. Left: shift in stop-band of 98 nm after hydrosilylation of undecenoic acid (2) and 38 nm after activation with *N*-hydroxysuccinimide and coupling of the tripeptide Gly-Gly-His (4). Right: transmission Fourier transform infra red spectra of the same rugate filter showing: (2) hydrosilylation of undecenoic acid, -C–H stretching of the alkyl chain at 2850–2920 cm^{-1}, Si–H_x stretching from the un-reacted surface at 2090 cm^{-1} and C═O stretching of the carboxylic acid at 1710 cm^{-1}, (3) reaction with NHS to yield the active ester shift in the carbonyl to 1740 cm^{-1}, new succinimide carbonyls at 1780/1820 cm^{-1}, N–O stretching at 1210 cm^{-1} and C–O stretching at 1070 cm^{-1}, (4) peptide immobilization: broad –OH stretching at 3320 cm^{-1} and amide bands at 1650/1540/1460 cm^{-1}.

penetrate into the structure while larger biomolecules are excluded. Such small pore sizes therefore potentially provides a methodology for reducing protein adsorption whilst selecting for analytes *via* size exclusion. For many applications however, larger pores are critical for sensing large analytes which led to the investigation of a material with higher doping density (0.005 Ω cm, *highly* doped) that has been shown to produce larger pores with a more uniform morphology.[17] The *highly* doped silicon rugate filters were found to allow easy infiltration of the large proteins but exhibit smaller shifts of the stop band due to the smaller ratio of surface area to pore volume,[15] similar to the findings of Fauchet and colleagues[72] that larger pores resulted in inferior optical properties. The stability and antifouling characteristics of the *highly* doped PSi structures demonstrated comparable resistance to non-specific adsorption but with even greater stability in biological solutions compared to the *medium* doped material.[12,14] From these studies we conclude for PSi with similar porosity that (1) smaller pores can result in larger optical responses upon changes in refractive index but may exhibit reduced stability and prevent large biomolecules from entering, (2) PSi with larger pores yields a smaller optical response but show higher stability and is more appropriate for work with large globular biomolecules. In all cases a robust surface chemistry is essential to protect the surface from degradation, resist non-specific adsorption and provide a flexible system that allows a variety of biorecognition moieties to be incorporated.

4.2 Opportunities for porous silicon biosensors and future directions

With robust stable surface chemistry that effectively passivates the porous silicon from rapid degradation in aqueous media, the possibilities for using PSi for biosensing appear considerable. The question arises though as to what are these possibilities? Two of the features of PSi photonic crystals which are instantly attractive for biosensing are (1) the sensitivity of their optical response to small changes in refractive index provides the potential for high sensitivity (for example Fauchet and co-workers demonstrated optical responses were observed with only 1–2% of a monolayer bound to the surface of a photonic crystal[10]) and (2) the nanoporous nature of the materials means that once biomolecules infiltrate into the PSi structure, diffusional pathlengths are short and hence response times should be rapid. There are however caveats to these two advantages. With the latter, rapid response times are only achieved once the analyte is within the nanoporous structure. Hence if the PSi pore space is filled with air, exposure to an aqueous sample that is drawn into the pores will see a rapid response. It is the rapid filling of an empty PSi structure that is responsible for the rapid response of the protease biosensor demonstrated by Sailor and co-workers.[9] However, if the PSi is already filled with solution, the analyte still must diffuse into the nanoporous structure and hence rapid response times are lost. In relation to the former, the sensitivity is compromised by the fact that even though as little as 1% or less of a monolayer of protein bound to the walls of the PSi pores can be detected, the incredibly high surface areas of these nanoporous structures means this 1% is still a large amount of protein. In our work on protease biosensing[7] we have overcome this requirement for large amount of material changing at the pore surfaces by exploiting the fact that each protease enzyme can cleave many peptides from the pore walls and hence low detection limits are achieved.

Two other less well recognised advantages of nanoporous materials for biosensing is the potential for using the pore size to selectively control what material enters the photonic crystal[14,23,83,99] and the ability of the structure to concentrate the analyte. We have utilized both these advantages in our recent work. In relation to concentrating analyte, this is demonstrated by the detection of cholera toxin using a hybrid lipid bilayer (hBLM) containing the ganglioside GM1 as the recognition species that was formed inside the pores of a rugate filter (Fig. 8(a)).[8] hBLMs are formed by fusion and unrolling of lipid vesicles onto a hydrophobic surface thus leaving the hydrophilic headgroup exposed to solution. This strategy provides a biomimetic interface for selecting multi-valent biomolecules not possible with covalent strategies and should prove amenable to other cell-targeting toxins by merely changing the headgroup of a lipid component. The dense alkyl monolayer beneath the lipid layer is extremely stable allowing reuse of the sensor chip by rinsing in ethanol and repeat application of vesicles. Using this biosensor as little as

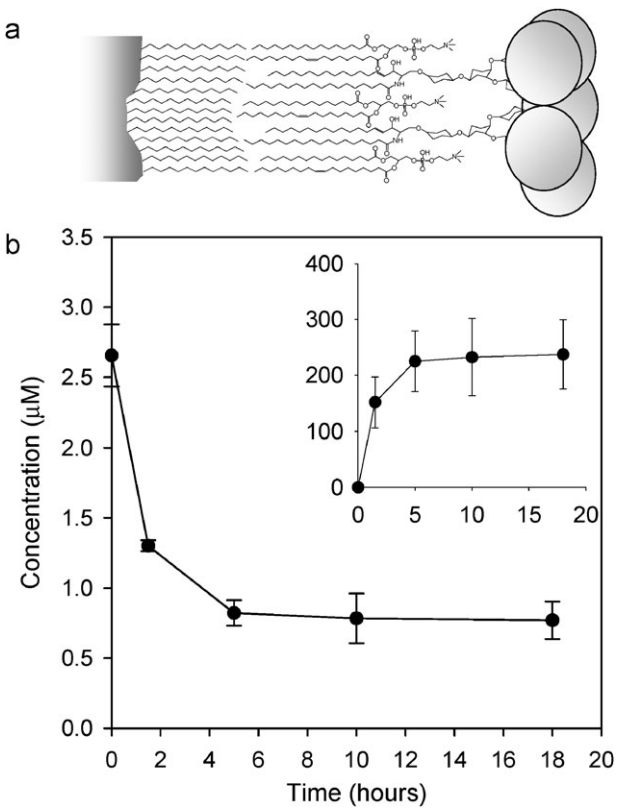

Fig. 8 (a) Hybrid lipid bilayer membrane assembled by deposition of small unilamellar vesicles containing phosphatidylcholine lipids and the cholera binding pentasaccharide GM1 onto the pore wall of a rugate filter modified by hydrosilylation of dodecene. (b) Reduction in cholera measured in solution above the PSi (^{125}I labelled). Inset: corresponding concentration within the nanoarchitecture (same axis labels, Figure adapted from ref. 8).

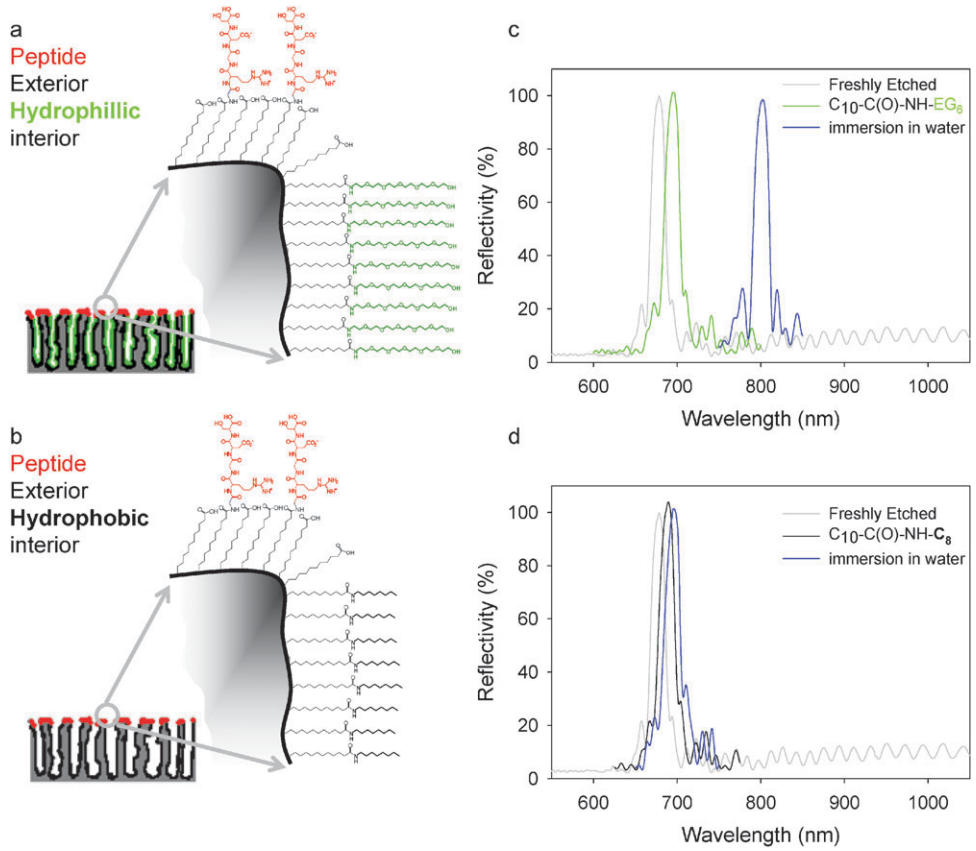

Fig. 9 (a) Depiction of a pore aperture modified on the top with the cell adhesive peptide GRGDS under aqueous conditions followed by internal modification with the hydrophilic EG_6 moiety in organic solvent. (b) Structure modified with the same external cell adhesive peptide but with a different internal (hydrophobic) monolayer created by immobilization of octylamine, (c) and (d) surfaces from (a) and (b) after immersion in water demonstrating the different photonic responses by allowing or preventing the ingress of water, respectively.

0.2 pmol of cholera in 200 μL was detected. Detection of this low amount of material was only possible because of the ability of the PSi to concentrate the analyte, Fig. 8(b) shows that with a cholera concentration of 3 μM, within 8 hours the concentration of cholera in the solution had decreased by $>70\%$ with an associated increase to over 200 μM within the photonic crystal (Fig. 8(b) inset). This property of PSi both enables concentration of analytes for identification (*i.e.* mass spectrometry) as well as the potential for "smart" remediation by optical detection of the concentration of toxins in a static device, flow-through system or by dispersing microparticles.

Photonic detection of biomolecules combined with size selectivity was exploited in a later application motivated towards detecting the release of material from cells adhered to the outer surface of the photonic crystal but unable to enter the pore space.[13] Crucial to this application is modifying the internal and the external surfaces of the photonic crystal with completely different chemistry. Fig. 9 show this strategy where the top of the PSi is modified by the cell adhesive peptide GRGDS while the interior is separately modified by a hydrophilic (a) and hydrophobic (b) molecule, respectively. This is possible because once the photonic crystal is modified with a relatively hydrohobic succinimide ester terminated base layer, aqueous peptide solution does not readily enter the nanoporous material. Hence only the external surface is modified with peptide. After derivatizing the top, the interior can be reacted using organic solvents that fully enter the pores. This is demonstrated in Fig. 9(c) and (d) where application of water to the PSi leads to a much larger shift of the stop-band when the interior is hydrophilic. Using this strategy, we showed the selective capture of cells on the top of the PSi with detection of released cellular material on the inside thus paving the way to monitoring cellular secretion. Another interesting potential application for differentially modified PSi is for "smart" drug delivery[100] and monitoring the viability of adherent cells.[13,101]

Conclusions

The role of pore size and morphology on biosensor sensitivity is critical and should be modified as necessary depending on the analyte identity, mode of biorecognition, experiment timescale, solution conditions and format (*i.e.* laboratory, point-of-care). The sensitivity of the PSi rugate filters to refractive index changes can be adjusted by tuning the pore size. The larger the pores, the lower the sensitivity and thus etching parameters must be chosen to accommodate the analyte of interest whilst maximising the optical response to refractive index changes. Thus careful selection of anodisation parameters and surface modification strategy is important to ensure the best material to suit the application.

In addition, the selection of surface chemistry should be flexible and allow modification depending on the application.

Employing hydrosilylation chemistry with antifouling EG moieties gives the PSi enhanced stability and will thus be more amenable to prolonged biosensing experiments or *in vivo*/*ex vivo* diagnostics and biomaterials. In combination with surface chemistry and nanoarchitecture, choosing the target analyte (*e.g.* enzymatic activity) such that biorecognition capitalizes on the strengths of the transducer can further maximise device sensitivity. In summary, understanding the structure and surface chemistry of PSi is essential to choosing the right material for the experimental requirements.

Notes and references

1 A. Uhlir, *Bell Syst. Technol. J.*, 1956, **35**, 333.
2 L. T. Canham, *Appl. Phys. Lett.*, 1990, **57**, 1046.
3 L. T. Canham, *Adv. Mater.*, 1995, **7**, 1033–1037.
4 G. Vincent, *Appl. Phys. Lett.*, 1994, **64**, 2367–2369.
5 V. S. Y. Lin, K. Motesharei, K.-P. S. Dancil, M. J. Sailor and M. R. Ghadiri, *Science*, 1997, **278**, 840–843.
6 S. Chan, S. R. Horner, P. M. Fauchet and B. L. Miller, *J. Am. Chem. Soc.*, 2001, **123**, 11797–11798.
7 K. A. Kilian, T. Böcking, K. Gaus and J. J. Gooding, *ACS Nano*, 2007, **1**, 355–361.
8 K. A. Kilian, T. Böcking, K. Gaus, J. King-lacroix, M. Gal and J. J. Gooding, *Chem. Commun.*, 2007, 1936–1938.
9 M. M. Orosco, C. Pacholski, G. M. Miskelly and M. J. Sailor, *Adv. Mater.*, 2006, **18**, 1393–1396.
10 H. Ouyang, M. Christophersen, R. Viard, B. L. Miller and P. M. Fauchet, *Adv. Funct. Mater.*, 2005, **15**, 1851–1859.
11 C. Pacholski, M. Sartor, M. J. Sailor, F. Cunin and G. M. Miskelly, *J. Am. Chem. Soc.*, 2005, **127**, 11636–11645.
12 K. A. Kilian, T. Böcking, K. Gaus, M. Gal and J. J. Gooding, *Biomaterials*, 2007, **28**, 3055–3062.
13 K. A. Kilian, T. Böcking, K. Gaus and J. J. Gooding, *Angew. Chem., Int. Ed.*, 2008, **47**, 2697–2699.
14 K. A. Kilian, T. Böcking, S. Ilyas, K. Gaus, M. Gal and J. J. Gooding, *Adv. Funct. Mater.*, 2007, **17**, 2884–2890.
15 K. A. Kilian, T. Böcking, L. M. H. Lai, S. Ilyas, K. Gaus, M. Gal and J. J. Gooding, *Int. J. Nanotechnol.*, 2007, **5**, 170–178.
16 A. G. Cullis, L. T. Canham and P. D. J. Calcott, *Appl. Phys. Rev.*, 1997, **82**, 909–956.
17 V. Lehmann, R. Stengl and A. Luigart, *Mater. Sci. Eng. B*, 2000, **69–70**, 11–22.
18 H. Foll, M. Christophersen, J. Carstensen and G. Hasse, *Mater. Sci. Eng. R*, 2002, **39**, 93–141.
19 W. Theiss, *Surf. Sci. Rep.*, 1997, **29**, 91–192.
20 P. Allongue, V. Costa-Kieling and H. Gerischer, *J. Electrochem. Soc.*, 1993, **140**, 1018–1026.
21 I. N. Lees, H. Lin, C. A. Canaria, C. Gurtner, M. J. Sailor and G. M. Miskelly, *Langmuir*, 2003, **19**, 9812–9817.
22 J. E. Bateman, B. R. Horrocks and A. Houlton, *J. Chem. Soc., Faraday Trans.*, 1997, **93**, 2427–2431.
23 B. E. Collins, K.-P. S. Dancil, G. Abbi and M. J. Sailor, *Adv. Funct. Mater.*, 2002, **12**, 187–191.
24 M. Archer, M. Christophersen and P. M. Fauchet, *Biomed. Microdevices*, 2004, **6**, 203–211.
25 S. Chan, P. M. Fauchet, Y. Li and L. J. Rothberg, *Proc. SPIE*, 2000, **3912**, 23–34.
26 C. Steinem, A. Janshoff, V. S. Y. Lin, N. H. Voelcker and M. Reza Ghadiri, *Tetrahedron*, 2004, **60**, 11259–11267.
27 L. M. Bonanno and L. A. DeLouise, *Langmuir*, 2007, **23**, 5817–5823.
28 K.-P. S. Dancil, D. P. Greiner and M. J. Sailor, *J. Am. Chem. Soc.*, 1999, **121**, 7925–7930.
29 M. P. Schwartz, S. D. Alvarez and M. J. Sailor, *Anal. Chem.*, 2007, **79**, 327–334.
30 P. S. Chaudhari, A. Gokarna, M. Kulkarni, M. S. Karve and S. V. Bhoraskar, *Sens. Actuators, B*, 2005, **107**, 258–263.
31 S. E. Letant, B. R. Hart, S. R. Kane, M. Z. Hadi, S. J. Shields and J. G. Reynolds, *Adv. Mater.*, 2004, **16**, 689–693.
32 S. E. Letant, S. R. Kane, B. R. Hart, M. Z. Hadi, T.-C. Cheng, V. K. Rastogi and J. G. Reynolds, *Chem. Commun.*, 2005, 851–853.
33 R. R. K. Reddy, A. Chadha and E. Bhattacharya, *Biosens. Bioelectron.*, 2001, **16**, 313–317.
34 D. Olmos, J. Gonzalez-Benito, A. J. Aznar and J. Baselga, *J. Mater. Process. Technol.*, 2003, **143–144**, 82–86.
35 J. M. Buriak, *Chem. Rev.*, 2002, **102**, 1271–1308.
36 M. R. Linford and C. E. D. Chidsey, *J. Am. Chem. Soc.*, 1993, **115**, 12631–12632.
37 M. R. Linford, P. Fenter, P. M. Eisenberger and C. E. D. Chidsey, *J. Am. Chem. Soc.*, 1995, **117**, 3145–3155.
38 J. M. Buriak, *Adv. Mater.*, 1999, **11**, 265–267.
39 R. Boukherroub, S. Morin, D. D. M. Wayner, F. Bensebaa, G. I. Sproule, J. M. Baribeau and D. J. Lockwood, *Chem. Mater.*, 2001, **13**, 2002–2011.
40 R. Boukherroub, D. D. M. Wayner and D. J. Lockwood, *Appl. Phys. Lett.*, 2002, **81**, 601–603.
41 R. Boukherroub, D. D. M. Wayner, G. I. Sproule, D. J. Lockwood and L. T. Canham, *Nano Lett.*, 2001, **1**, 713–717.
42 R. Boukherroub, J. T. C. Wojtyk, D. D. M. Wayner and D. J. Lockwood, *J. Electrochem. Soc.*, 2002, **149**, H59–H63.
43 J.-N. Chazalviel, C. Vieillard, M. Warntjes and F. Ozanam, *Proc. Electrochem. Soc.*, 1996, **118**, 5375–5382.
44 B. Gelloz, H. Sano, R. Boukherroub, D. D. M. Wayner, D. J. Lockwood and N. Koshida, *Phys. Status Solidi C*, 2005, **2**, 3273–3277.
45 J. T. C. Wojtyk, K. A. Morin, R. Boukherroub and D. D. M. Wayner, *Langmuir*, 2002, **18**, 6081–6087.
46 J. M. Schmeltzer, J. Lon A. Porter, M. P. Stewart and J. M. Buriak, *Langmuir*, 2002, **18**, 2971–2974.
47 E. J. Lee, T. W. Bitner, J. S. Ha, M. J. Shane and M. J. Sailor, *J. Am. Chem. Soc.*, 1996, **118**, 5375–5382.
48 M. P. Stewart and J. M. Buriak, *J. Am. Chem. Soc.*, 2001, **123**, 7821–7830.
49 R. Boukherroub, A. Petit, A. Loupy, J.-N. Chazalviel and F. Ozanam, *J. Phys. Chem. B*, 2003, **107**, 13459–13462.
50 J. M. Buriak and M. J. Allen, *J. Am. Chem. Soc.*, 1998, **120**, 1339–1340.
51 J. M. Buriak, M. P. Stewart, T. W. Geders, M. J. Allen, H. C. Choi, J. Smith, D. Raftery and L. T. Canham, *J. Am. Chem. Soc.*, 1999, **121**, 11491–11502.
52 J. M. Buriak and M. J. Allen, *J. Lumin.*, 1999, **80**, 29–35.
53 J. M. Holland, M. P. Stewart, M. J. Allen and J. M. Buriak, *J. Solid State Chem.*, 1999, **147**, 251–258.
54 M. Rocchia, S. Borini, A. M. Rossi, L. Boarino and G. Amato, *Adv. Mater.*, 2003, **15**, 1465–1469.
55 J. H. Song and M. J. Sailor, *J. Am. Chem. Soc.*, 1998, **120**, 2376–2381.
56 N. Y. Kim and P. E. Laibinis, *J. Am. Chem. Soc.*, 1998, **120**, 4516–4517.
57 I. N. Lees, H. Lin, C. A. Canaria, C. Gurtner, M. J. Sailor and G. M. Miskelly, *Langmuir*, 2003, **19**, 9812–9817.
58 E. G. Robins, M. P. Stewart and J. M. Buriak, *Chem. Commun.*, 1999, **24**, 2479–2480.
59 L. H. Lie, S. N. Patole, A. R. Pike, L. C. Ryder, B. A. Connolly, A. D. Ward, E. M. Tuite, A. Houlton and B. R. Horrocks, *Faraday Discuss.*, 2004, **125**, 235–249 (*Faraday Discuss.*, 2004, **125**, 293–309) (Discussion).
60 B. R. Hart, S. E. Letant, S. R. Kane, M. Z. Hadi, S. J. Shields and J. G. Reynolds, *Chem. Commun.*, 2003, 322–323.
61 A. Janshoff, K.-P. S. Dancil, C. Steinem, D. P. Greiner, V. S. Y. Lin, C. Gurtner, K. Motesharei, M. J. Sailor and M. R. Ghadiri, *J. Am. Chem. Soc.*, 1998, **120**, 12108–12116.
62 L. D. Stefano, L. Rotiroti, I. Rea, L. Moretti, G. D. Francia, E. Massera, A. Lamberti, P. Arcari, C. Sanges and I. Rendina, *J. Opt. A*, 2006, **8**, S540–S544.
63 S. D'Auria, M. d. Champdore, V. Aurilia, A. Parracino, M. Staiano, A. Vitale, M. Rossi, H. Rea, L. Rotiroti, A. M. Rossi, S. Borini, I. Rendina and L. D. Stefano, *J. Phys. Condens. Matter.*, 2006, **18**, S2019–S2028.
64 L. D. Stefano, M. Rossi, M. Staiano, G. Mamone, A. Parracino, L. Rotiroti, I. Rendina, M. Rossi and S. D'Auria, *J. Proteome Res.*, 2006, **5**, 1241–1245.

65 A. M. Tinsley-Bown, R. G. Smith, S. Hayward, M. H. Anderson, L. Koker, G. A. R. Torrens, A.-S. Wilkinson, E. A. Perkins, D. J. Squirrell, S. Nicklin, A. Hutchinson, A. J. Simons and T. I. Cox, *Phys. Status Solidi A*, 2005, **202**, 1347–1356.
66 C. Mazzoleni and L. Pavesi, *Appl. Phys. Lett.*, 1995, **67**, 2983–2985.
67 P. J. Reece, M. Gal, H. H. Tan and C. Jagadish, *Appl. Phys. Lett.*, 2004, **85**, 3363–3365.
68 P. J. Reece, G. Lerondel, W. H. Zheng and M. Gal, *Appl. Phys. Lett.*, 2002, **81**, 4895–4897.
69 L. A. DeLouise and B. L. Miller, *Anal. Chem.*, 2005, **77**, 1950–1956.
70 L. D. Stefano, I. Rea, I. Rendina, L. Rotiroti, M. Rossi and S. D'Auria, *Phys. Status Solidi A*, 2006, **203**, 886–891.
71 H. Ouyang, L. A. DeLouise, B. L. Miller and P. M. Fauchet, *Anal. Chem.*, 2007, **79**, 1502–1506.
72 H. Ouyang, C. C. Striemer and P. M. Fauchet, *Appl. Phys. Lett.*, 2006, **88**, 163108.
73 S. Ilyas, T. Böcking, K. Kilian, P. J. Reece, J. Gooding, K. Gaus and M. Gal, *Opt. Mater.*, 2007, **29**, 619–622.
74 E. Lorenzo, J. Oton Claudio, E. Capuj Nestor, M. Ghulinyan, D. Navarro-Urrios, Z. Gaburro and L. Pavesi, *Appl. Opt.*, 2005, **44**, 5415–5421.
75 E. Lorenzo, C. J. Oton, N. E. Capuj, M. Ghulinyan, D. Navarro-Urrios, Z. Gaburro and L. Pavesi, *Phys. Status Solidi A*, 2005, **2**, 3227–3231.
76 M. J. Sailor and J. R. Link, *Chem. Commun.*, 2005, 1375–1383.
77 F. Cunin, T. A. Schmedake, J. R. Link, Y. Y. Li, J. Koh, S. N. Bhatia and M. J. Sailor, *Nat. Mater.*, 2002, **1**, 39–41.
78 E. J. Anglin, M. P. Schwartz, V. P. Ng, L. A. Perelman and M. J. Sailor, *Langmuir*, 2004, **20**, 11264–11269.
79 J. S. Park, S. O. Meade, E. Segal and M. J. Sailor, *Phys. Status Solidi A*, 2007, **204**, 1383–1387.
80 J. R. Dorvee, A. M. Derfus, S. N. Bhatia and M. J. Sailor, *Nat. Mater.*, 2004, **3**, 896–899.
81 J. C. Thomas, C. Pacholski and M. J. Sailor, *Lab Chip*, 2006, **6**, 782–787.
82 J.-H. Park, A. M. Derfus, E. Segal, K. S. Vecchio, S. N. Bhatia and M. J. Sailor, *J. Am. Chem. Soc.*, 2006, **128**, 7938–7946.
83 L. Gao, N. Mbonu, L. Cao and D. Gao, *Anal. Chem.*, 2008, **80**, 1468–1473.
84 T. Böcking, M. Gal, K. Gaus and J. J. Gooding, *Aust. J. Chem.*, 2005, **58**, 660–663.
85 T. Böcking, K. A. Kilian, K. Gaus and J. J. Gooding, *Langmuir*, 2006, **22**, 3494–3496.
86 T. Böcking, K. A. Kilian, T. Hanley, S. Ilyas, K. Gaus, M. Gal and J. J. Gooding, *Langmuir*, 2005, **21**, 10522–10529.
87 T. L. Clare, B. H. Clare, B. M. Nichols, N. L. Abbott and R. J. Hamers, *Langmuir*, 2005, **21**, 6344–6355.
88 M. P. Schwartz, F. Cunin, R. W. Cheung and M. J. Sailor, *Phys. Status Solidi A*, 2005, **202**, 1380–1384.
89 C. M. Yam, J. M. Lopez-Romero, J. Gu and C. Cai, *Chem. Commun.*, 2004, 2510–2511.
90 T. Böcking, S. Ilyas, G. P. Salvador, P. J. Reece, K. Gaus, J. J. Gooding and M. Gal, in *Proceedings of COMMAD 2004, Conference on Optoelectronic and Microelectronic Materials and Devices*, IEEE, Brisbane, Australia, December 8–10, 2004, pp. 217–220.
91 Y.-L. Khung, S. D. Graney and N. H. Voelcker, *Biotechnol. Prog.*, 2006, **22**, 1388–1393.
92 L. Tay, N. L. Rowell, D. J. Lockwood and R. Boukherroub, *J. Vac. Sci. Technol.*, 2006, **24**, 747–751.
93 L. Tay, N. L. Rowell, D. Poitras, J. W. Fraser, D. J. Lockwood and R. Boukherroub, *Can. J. Chem.*, 2004, **82**, 1545–1553.
94 K. A. Kilian, T. Böcking, S. Ilyas, K. Gaus, M. Gal and J. J. Gooding, in *Proceedings of ICONN 2006, International Conference on Nanoscience and Nanotechnology*, IEEE, Brisbane, Australia, July 3–7 2006, pp. 486–488.
95 T. Böcking, K. A. Kilian, K. Gaus and J. J. Gooding, *Adv. Funct. Mater.*, in press.
96 S. Ciampi, T. Böcking, K. A. Kilian, M. James, J. B. Harper and J. J. Gooding, *Langmuir*, 2007, **23**, 9320–9329.
97 S. Ciampi, T. Böcking, K. A. Kilian, J. B. Harper and J. J. Gooding, *Langmuir*, 2008, **24**, 5888–5892.
98 S. Ciampi, G. Le Saux, J. B. Harper and J. J. Gooding, *Electroanalysis*, 2008, **20**, 1513–1519.
99 M. M. Orosco, C. Pacholski, G. M. Miskelly and M. J. Sailor, *Adv. Mater.*, 2006, **18**, 1393–1396.
100 E. J. Anglin, L. Cheng, W. R. Freeman and M. J. Sailor, *Adv. Drug Delivery Rev.*, 2008, **60**, 1266–1277.
101 M. P. Schwartz, A. M. Derfus, S. D. Alvarez, S. N. Bhatia and M. J. Sailor, *Langmuir*, 2006, **22**, 7084–7090.

